EXPERIMENTAL FLOW BOILING STUDY IN A 0.52 MM DIAMETER VERTICAL TUBE USING R134A

D. Shiferaw, M.M. Mahmoud, T.G. Karayiannis and D.B.R. Kenning

School of Engineering and Design, Brunel University, West London,
Uxbridge, Middlesex, UB8 3PH, UK, email:tassos.karayiannis@brunel.ac.uk

Abstract

Experimental results for R134a boiling on a vertical stainless steel tube of internal diameter 0.52 mm are presented in this paper. They form part of an ongoing study of flow boiling in a wide range of small diameter tubes. Other parameters were varied in the range: mass flux 300-700 kg/m^2.s; heat flux 1.6-75 kW/m^2 and pressure 6 -10 bar. The flow patterns visualised at the exit of the heated test section are first presented. The variation of the heat transfer coefficient with thermodynamic quality and its dependence on heat flux, mass flux and system pressure is then presented and discussed.

Nomenclature

D	internal diameter, (m)		***Greek Symbols***	
G	mass flux, (kg/m² s)	α	heat transfer coefficient, (W/m²	
h_{lv}	latent heat of vaporization (J/kg)	Δ	change	
k	thermal conductivity (W/m·K)	ΔT_{sat}	degree of wall superheat (T_w-T_{sat})	
L	length, m	ρ	density, (kg/m³)	
m	mass flow rate, (kg/s)		***Subscripts***	
Nu	Nusselt number,	i	inside	
P	pressure, bar	l	liquid	
q	Heat flux, (W/m²)	o	outer	
Q	total heat, (W)	sat	saturation	
T	temperature, (^{0}C)	v	vapour	
x	vapour quality	w	wall	
z	axial distance	0	initial	

1   Introduction

Two-phase boiling in very small diameter tubes is one of the promising methods considered for cooling of high power electronics circuits and fundamental boiling heat transfer data is required for the understanding of the heat transfer mechanism and the development of accurate design methods for thermal management of micro-devices. Hence, intensive research is focussed on flow boiling in very small diameter tubes and there are a lot of experimental results from various sources. However, there is still scattering in the available heat transfer data and different conclusions on the prevailing heat transfer mechanisms are reported. This is probably due to the different experimental conditions and methodologies employed by researchers, added to the experimental uncertainties associated with data collecting. Therefore, an extensive study of flow patterns, heat transfer and pressure drop under the same conditions covering a wide range of diameters and other parameters was necessary in order to address the above issues. The experimental heat transfer and flow pattern results and comparison with correlations and models for 4.26, 2.01 and 1.10 mm diameter tubes

have been presented in various conferences and journals, Huo et al. (2007), Chen et al. (2006), Shiferaw et al. (2007). The present study is an extension of these works to a 0.52 mm diameter tube.

Experimental results for small diameter tubes demonstrated heat transfer coefficients that were more or less independent of vapour quality and mass flux, but strongly dependent on heat flux and saturation pressure, (Lazarek and Black (1982), Tran et al. (1996), Bao et al. (2000), Huo et al. (2007)). Conventionally, this is interpreted as evidence that nucleate boiling is the dominant heat transfer mechanism. However, using macroscale boiling heat transfer correlations based on the above premise did not predict well the heat transfer coefficient in small diameters, (Qu and Mudawar (2003) and Huo et al. (2007)). On the other hand, models based on convective evaporation of elongated bubbles were observed to predict small diameter tube heat transfer results better than empirical correlations (Dupont et al. (2004), Shiferaw et al. (2007)). Furthermore, Dı´az and Schmidt (2007) investigated transient boiling heat transfer in 0.3 x 12.7 mm microchannels using infrared thermography to measure the wall temperature. For water, the heat transfer coefficient decreased with quality near the zero quality region followed by a uniform heat transfer coefficient. However, for ethanol, at high quality, an increase in heat transfer coefficient with quality was found to be independent of applied heat flux. A similar behaviour was observed by Xu et al. (2005) and Lin et al. (2001) both of whom suggested a convective boiling dominant effect. Others have also reported combined effect of both mechanisms, i.e. nucleate boiling at low quality and forced convective boiling at high quality region, (Sumith et al. (2003), Saitoh et al. (2005)).

Flow boiling in very small diameter tubes is usually associated with high initial liquid superheat required to initiate boiling. Yen et al. (2003) conducted flow boiling experiments in 0.19, 0.3 and 0.51 mm inside diameter tubes using R123 and FC-72. They observed a high liquid superheat that reached up to 70 K in their experiments. In the low quality region, the heat transfer coefficient was observed to decrease with quality up to approximately x = 0.25 and then became almost constant with further increase in quality. Hapke et al. (2000) investigated experimentally convective boiling in a 1.5 mm internal diameter tube and reported that the onset of boiling occurred at higher liquid superheat than required for convectional tubes. The unusual superheat in micro tubes was also reported to be related to the reduction of active nucleation sites and vapour nucleation inside very small channels, (Zhang et al. (2001) and Brereton (1998)). In this paper, experimental results from several boiling test inside a 0.52 mm stainless steel tube are presented. Parallel visualization of the flow was also made at the exit to the heating section.

2 Experimental Facility and Procedure

An experimental facility was constructed during the early part of this study to determine the heat transfer coefficient in small diameter tubes using R134a fluid. A detailed description and a schematic diagram are available in Huo et al. (2007). The test section was a stainless steel cold drawn tube of internal diameter 0.52 mm, heated length 100 mm, wall thickness 0.15 mm. Direct electric heating was applied to the test section; ten K-type thermocouples were soldered to the outside of the tube at equal distances to provide the wall temperatures. T-type thermocouples and pressure transducers were used to measure inlet and outlet temperatures and pressures. All the instruments used were carefully calibrated. The uncertainty in temperature measurement was ± 0.15 K, flow rate measurements ± 0.4%, and pressure measurements ± 0.15 %. The diameter was measured within 2.8 % accuracy.

A series of flow boiling heat transfer tests were performed for R134a in the 0.52 mm tube for conditions in the range: pressure 6 to 10 bar, heat flux 1.6-75 kW/m^2, mass flux 300-700 kg/m^{2}s, vapour quality 0-0.9. The fluid inlet temperature was kept between 1 K and 5 K below saturation and the heat flux was increased in steps until the exit quality reached about 90% at fixed mass flux

and system pressure. The data were recorded after the system was steady. Each recording was the average of 20 measurements. A Pyrex glass tube for flow pattern observation was located immediately downstream of the heat transfer test section. A digital high-speed camera (Phantom V4 B/W, 250 x 512 pixels resolution, 1900 pictures/sec) was used to observe the flow patterns. The local heat transfer coefficient at each thermocouple point was determined based on the following equation,

$$\alpha = \frac{q}{T_{wi} - T_l} \qquad (1)$$

where T_w is the local inner wall temperature, T_l is the local fluid temperature and q is the inner wall heat flux to the fluid. T_l was deduced from the fluid pressure, which was determined based on the assumption of a linear pressure drop through the test section. The inside wall temperature, T_{wi}, can be determined using the internal heat generation and radial heat conduction across the tube wall. The experimental uncertainty in determining α is $\pm$ 12.5%. The heat flux was calculated from the product of the current and voltage across the tube minus the losses to the ambient. An energy balance based on the heat supplied minus losses and the enthalpy change enabled the thermodynamic quality (x_i) to be calculated.

$$x_i = \frac{h_i - h_l}{h_{lv}} \qquad (2)$$

where h_l and h_v are the specific enthalpy of saturated liquid and vapour, respectively. h_i is the local specific enthalpy of the fluid. This was determined from the enthalpy of the previous section and the heat transferred to the fluid, i.e.

$$h_i = h_{i-1} + \frac{L_i}{mL}(Q - \Delta Q) \qquad (3)$$

where as stated above, the heat input (Q) is equal to the product of the voltage and the current applied directly to the test section. The heat lost to the ambient, ΔQ, was estimated from measurements of the outer temperature of the insulation round the test section, calibrated against heat loss by heat balances during single-phase experiments, conducted prior to each boiling test at the same condition, see also Huo et al. (2007).

Comparisons of the single phase Nusselt number for the 0.52 mm tube with various well-known correlations both for turbulent and laminar flow are shown in Figures 1 and 2. The modified Gnielnsk (1997) correlation accounts for both transition region and developing effects; the Adams et al. (1998) correlation is a modification of the Gnielnski correlation to accommodate the small diameter effect. In the laminar regime the experimental results were compared with the Peng and Peterson (1996) correlation for rectangular micrchannels and the Choi et al. (1991) correlation for microtubes. The results agree quite well with modified Gnielinski (1997) and Adams et al. (1998) for the turbulent regime and Choi et al. (1991) in the laminar regime. This validates the experimental methodology and provides reasonable confidence towards the two-phase experiments. In the turbulent region Dittus-Boelter and Petukhov did not match the experimental data probably because of the fact that both were developed for Re > 10000, while the other correlations can work down to the transition region. In the laminar region, the Peng and Peterson correlation is a function of channel aspect ratio. Consequently, the large deviation from the experimental data may be attributed to the effect of geometry.

In previous experiments with tubes in the size range 4.26 mm – 1.1 mm, boiling in bubbly flow was initiated at low heat fluxes of about 13 kW/m^2. The heat flux was then increased from this value to obtain the other test cases. In the tests with the 0.52 mm tube, this heat flux led to immediate boiling in the churn-annular regime. Consequently, a different procedure was employed.
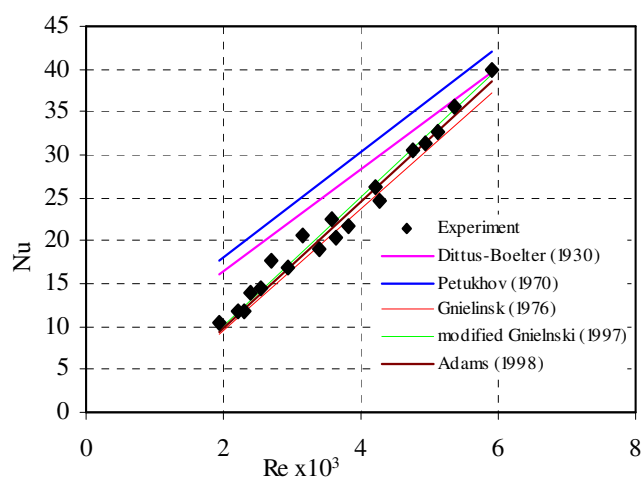
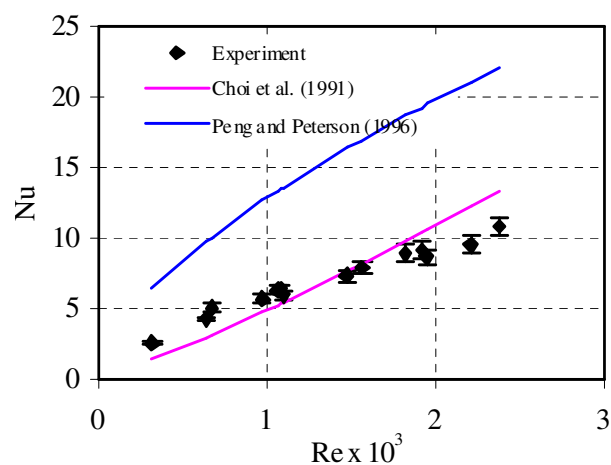Figure 1. *Single phase heat transfer for turbulent region*

Figure 2. *Single phase heat transfer for laminar region*

The heat flux was increased from single phase flow until confined bubble flow was observed in the glass tube at the exit from the test section. Despite the presence of bubbles, the thermocouple in the fluid at the exit recorded a temperature above the saturation temperature. Boiling was then maintained as the heat flux was reduced to a much lower value corresponding to bubbly flow, which was used as the starting point for the experiments with stepwise increases in heat flux.

3   Experimental Results and Discussion

3.1 Flow pattern visualization

Figure 3 presents the flow patterns observed during the boiling test at a mass flux of 300 kg/m^{2}s and pressure 6 bar. These flow patterns were taken simultaneously with the heat transfer tests presented in section 3.2 below at each value of heat flux. Confined bubble flow is observed at low heat flux or exit quality. As the heat flux increased, the bubbles grew in length and become elongated. Further increase in heat flux resulted in the liquid slug between the bubbles being "pushed" on to the upstream bubble creating coalescence of the bubbles and a wavy film (nos 6-7). A similar phenomenon was observed by Revellin et al. (2006). Figure 4 shows how three relatively short bubbles coalesce together to form an elongated bubble leaving the film interface wavy. As shown in figure 3, a further increase in heat flux makes the film interface wavy and highly non-uniform (e.g. flow pattern photo numbers 6-8). This could lead to a transition to annular flow, since further increase in heat flux reduces the wave irregularity and distributes the waves almost uniformly. At high heat flux, the flow pattern becomes annular with small-scale roughness of very short amplitude and wavelength. Chen et al. (2006) examined the flow patterns at qualities x > 0 leaving tubes of diameter from 4.26 mm down to 1.1 mm for R134a over the pressure range 6-14 bar. They defined the conventional regimes of dispersed bubble, bubbly, slug, churn, annular and annular-mist flow. However, in the current flow patterns for the 0.52 mm tube, dispersed bubble flow was not observed, while there was a liquid ring flow possibly as transition regime from slug to annular flow.

3.2 Heat transfer characteristics

The experimental local heat transfer coefficient is plotted as a function of quality in Figure 5 at a mass flux of 300 kg/m^{2}s and 6 bar system pressure. The flow patterns of figure 3 are the corresponding observations for heat flux values 14.8 to 58.4 kW/m^2 of these tests. The liquid-only Reynolds number is 720, which should correspond to laminar flow at the inlet. As seen in the figure, the experimental values demonstrate a varying dependence of the heat transfer coefficient on heat flux and thermodynamic vapour quality.
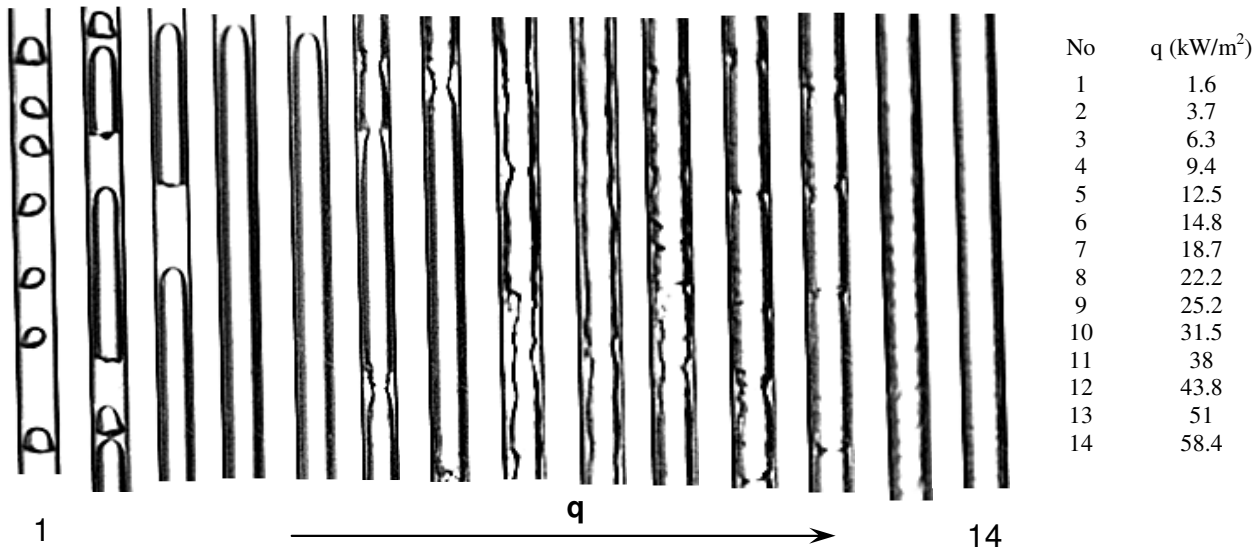
No	q (kW/m^2)
1	1.6
2	3.7
3	6.3
4	9.4
5	12.5
6	14.8
7	18.7
8	22.2
9	25.2
10	31.5
11	38
12	43.8
13	51
14	58.4

Figure 3. Flow patterns as a function of heat flux, G = 300 kg/m^{2}s, P = 6 bar.

Two groups exhibiting different influences of heat flux are observed below and above a heat flux of 14.8 kW/m^2. At the low heat fluxes, the heat transfer coefficient is higher at low vapour quality and drops sharply with quality, followed by a weak monotonic increase. Also, the heat transfer coefficient does not depend on heat flux. These results exhibit similar trend and range of heat transfer coefficient values with the R123 experimental results conducted by Yen et al. (2003) for 0.51 mm diameter, mass flux of 295 kg/m^{2}s and heat flux values of (q≤12.3 kW/m^2). There is an abrupt increase in the heat transfer coefficient and a change in its trend with quality and heat flux at heat fluxes of 14.8 kW/m^2 and above, for which there are different trends in four regions indicated by broken lines in figure 5 for the sake of lucidity and ease of comparison with later graphs at

Figure 4. *Sequence of flow patterns showing coalescence, G=300 kg/m^{2}s, P=6 bar and q =3.7 kW/m^2*

a

different mass flux. The regions become clearer at higher heat flux values. Lin et al. (2001) for 1 mm tube using R141b (for heat flux value less than 60 kW/m^2) and Dı´az and Shmidt (2007) for 0.3 x 12.7 mm rectangular channel using ethanol observed similar behaviour to this second group. Regions I - IV correspond respectively to trends of increase, uniform, decrease and a slight monotonic increase of heat transfer coefficient with thermodynamic quality. The classification will be used throughout the paper only for describing various features and identifying effects of parameters. The rapid increase in heat transfer coefficient with quality in Region I may be influenced by the inlet conditions, i.e. subcooled boiling effect and onset of nucleation. In region II, the heat transfer coefficient is independent of quality but increases with heat flux, behaviour that is conventionally interpreted as evidence for a nucleate boiling dominant region. This changes suddenly to region III, in which the heat transfer coefficient decreases with increasing quality. The decrease in heat transfer observed in the present results is different from that of a continuous decrease, observed towards the test section exit in the larger tubes of this study. This could occur due to intermittent dryout, which might be related to flow regimes of large disturbances in laminar film. Although, the flow patterns in figure 3 were taken at the same condition in order to relate the flow structure with the heat transfer characteristics, it is not possible to link them directly and draw a clear conclusion. This is because of the fact that they are taken at the exit of the heated section, i.e.
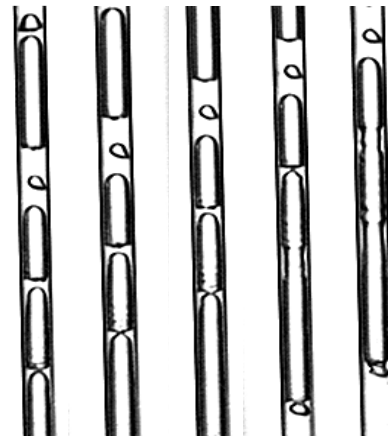
in the adiabatic section, and are liable to any flow regime development that might exist. After the 5th measuring thermocouple the heat transfer coefficient increases slightly with quality in region IV. In this region, the effect of heat flux is less at high quality. The continuous decrease of heat transfer coefficient with quality towards the test section exit that is observed at high heat flux in many tests with small diameter tubes, e.g. Huo et al. 2007, is not observed in the present experiments. This could be due to laminar flow and high surface tension force tending to coat the liquid along the circumference or small scale disturbances, which improve wetting of the wall. The wall superheat is plotted as a function of the heat flux in Figure 6 for different thermocouple positions (numbers in increasing order from inlet side) at a mass flux of 300 kg/m²s and 6 bar system pressure. As seen in the figure, for heat flux $q<\sim13$ kW/m², which corresponds to the first set of relatively low heat flux curves of figure 5, the degree of wall superheat increases rapidly with heat flux. This may be linked to the high wall superheat that was required to initiate boiling, indicating hysteresis in the activation of nucleation sites as a consequence of the smoothness or small size of the tube surface, Zhang et al (2001), Brereton (1998).
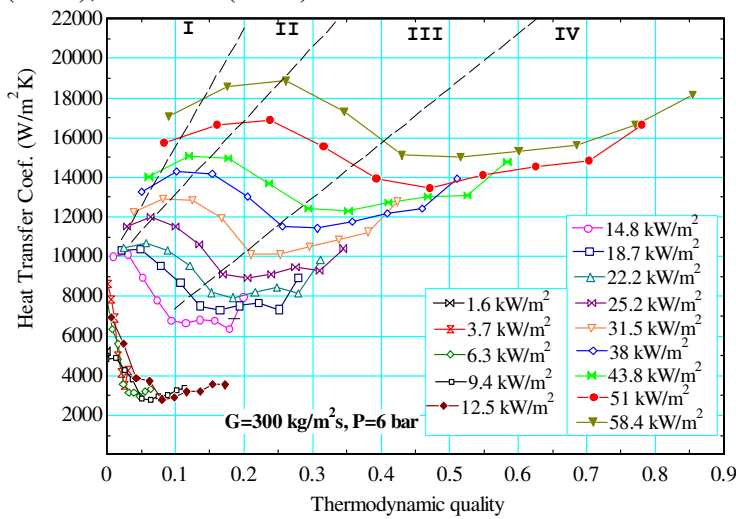

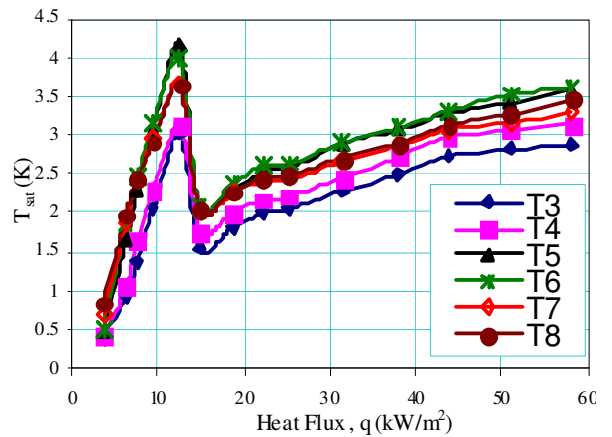Figure 5. *Heat transfer coefficient as a function of quality for G = 300 kg/m²s and P= 6 bar.*

Figure 6. *Degree of wall superheat as a function of heat flux for G= 300 kg/m²s, P=6 bar*

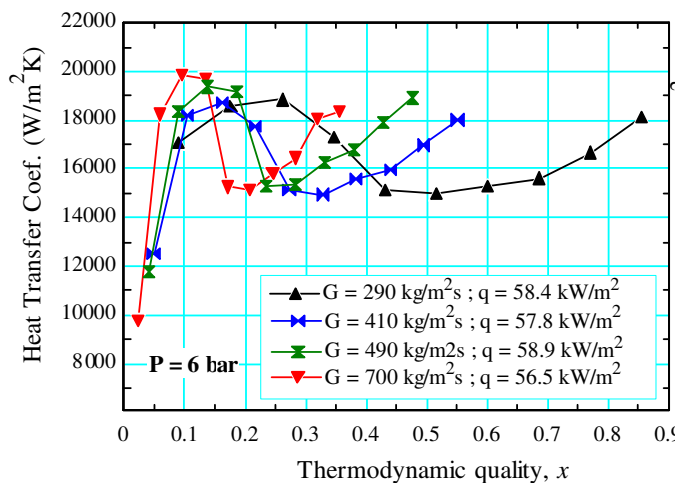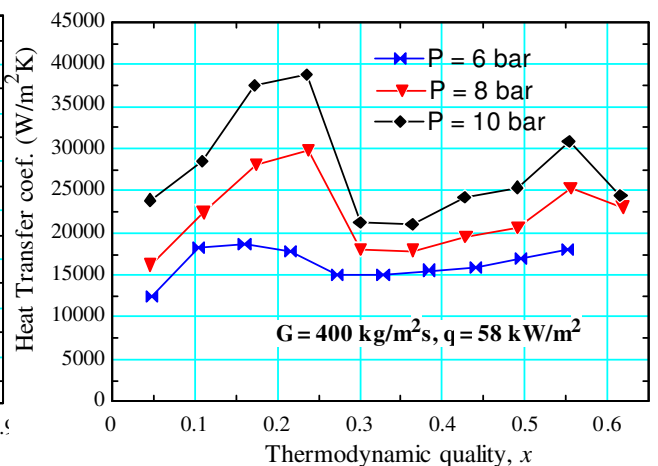Figure 7. *Effect of mass flux on heat transfer coefficient versus quality, $q_{nom} = 58$ kW/m²,*

Figure 8. *Effect of pressure on heat transfer coefficient versus quality, G = 400 kg/m²s, q = 58 kW/m²*

The superheating of the fluid at the exit from the test section gradually decreases as the heat flux increases. Beyond a heat flux of ~ 13 kW/m², the exit superheating disappears and there is a sudden decrease in the wall superheat. This is associated with a slight increase of system pressure and pressure drop.

The dependence of the heat transfer coefficient on mass flux is depicted in Figure 7 for a heat flux of 58 kW/m^2 and 6 bar pressure. As seen in the figure, there is a significant effect of mass flux in the region identified as IV (increasing trend of heat transfer coefficient with quality). In this region, the heat transfer coefficient increases with increasing mass flux; there is no obvious effect of heat flux especially at high quality (see figure 5). This plus the observations at the visualization section support the previous speculation that at high quality convective evaporation of the annular flow dominates the heat transfer mechanism, (Sumith et al (2003), Saitoh et al. (2005), Lin et al. (2001)). Also, the quality beyond which trend IV begins is lower at higher mass flux. There is a considerably smaller effect of mass flux in region I (increase of heat transfer coefficient with quality) and II (mostly uniform heat transfer coefficient with quality). However the length of region II decreases with increasing mass flux. (Refer to figure 5, for the different regions). The heat transfer coefficient is depicted as a function of quality for different system pressure in Figure 8 for a mass flux of 400 kg/m^{2}s and a heat flux of 58 kW/m^2. The heat transfer coefficient increases with system pressure. There is a drop in heat transfer coefficient at the last measuring point after the second maximum for 8 and 10 bar pressure, which might be caused by thin film dryout during the annular flow. It is also observed that for 6 bar, trend III (heat transfer coefficient decreasing with quality) is a gradual decrease compared to that at 8 and 10 bar, which showed a sudden drop from the 4th to the 5th measuring point, (x = 0.23 - 0.3).

4. Conclusions

A flow boiling experiment in a 0.52 mm tube internal diameter using R134a at pressures of 6 – 10 bar was conducted and representative flow patterns observed at the exit to the heating section and transfer results re presented. Dispersed bubble flow, observed in tests under similar conditions in larger tubes of 1.1 mm to 4.26 mm diameter, performed with the same facility was not observed, while ring flow was seen. The heat transfer results demonstrate patterns of dependence of the heat transfer coefficient on thermodynamic quality, heat flux and mass flux that change sharply in character at a threshold value of heat flux. Again these trends were not observed in tests for the larger tubes indicating a different behaviour for this tube. In the low heat flux region, there is no significant effect of heat flux but the heat transfer coefficient decreases and then increases slightly with thermodynamic quality. At moderate and high heat flux, in the front part of the channel, the heat transfer coefficient increases with increasing heat flux and reaches a maximum at an intermediate quality which might be caused by transient partial dryout or dry patches in the confined bubble regime. At higher quality, towards the test section exit, the heat transfer coefficient gradually increases again with quality but there is no clear effect of heat flux. The heat transfer coefficient increases with mass flux in this region. According to the conventional interpretation, this is evidence for a convective boiling dominant heat transfer mechanism in the annular flow region. The heat transfer coefficient increases with system pressure. At the higher pressures, there are indications of a second decrease in the heat transfer coefficient very close to the test section exit.

References

Adams T.M., Abdel-khalik S.I., Jeter S.M. and Qureshi Z.H., 1998, An Experimental Investigation of Single-Phase Forced Convection in Micro-Channels, Int. J. Heat Mass Transfer, Vol.41, No. 6-7, pp. 851-857.

Bao, Z. Y., Fletcher, D. F. and Haynes, B. S., 2000, Flow boiling heat transfer of Freon R11 and HCFC123 in narrow passages, Int. J. Heat Mass Transfer, Vol. 43, pp. 3347-3358.

Brereton, G.J., Crilly, R.J., Spears, J.R., 1998, Nucleation in small capillary tubes. Chem. Phys., Vol. 230, pp. 253–265.

Chen, L., Tian, Y.S. and Karayiannis, T.G., 2006, The effect of tube diameter on vertical two-phase flow regimes in small tubes, Int. J. Heat Mass Transfer, Vol. 49, pp. 4220-4230.

Choi, S.B. Barron, R.F. and Warrington, R.O., 1991, Fluid flow and heat transfer in microtubes, Micromechanical Sensors, Actuators and Systems, ASME DSC, Vol. 32, pp. 123–128.

Dı́az, M. C., Schmidt, J., 2007, Experimental investigation of transient boiling heat transfer in microchannels, Int. J. of Heat Fluid Flow, Vol. 28, pp. 95–102.

Dittus F.W. and Boelter L.M.K., 1930, Heat transfer in automobile radiators of tubular type, Univ. California Berkeley, Publ. Eng. 2/13, pp. 443–461.

Dupont, V., Thome, J. R., Jacobi, A.M., 2004, Heat transfer model for evaporation in microchannels, Part II: Comparison with the database, Int. J. Heat Mass Transfer, Vol. 47, pp. 3387-3401.

Gnielinski, V., 1976, New equations for heat transfer in turbulent pipe and channel flow. Int. Chem. Eng. 16, pp. 359–368.

Hapke, I., Boye, H., Schmidt, J., 2000, Onset of nucleate boiling in minichannels, Int. J. Therm. Sci. 39, pp. 505–513.

Huo X., Tian, Y.S., Karayiannis, T.G., 2007, R134a Flow boiling heat transfer in small diameter tubes, Advances in compact heat exchangers, R.T. Edwards, Inc., chapter 5, pp 95-111.

Lazarek, G. M. and Black, S. H., 1982, Evaporative heat transfer, pressure drop and critical heat flux in a small vertical tube with R-113, Int. J. Heat Mass Transfer, Vol. 25, No. 7, pp. 945-960.

Lin, S., Kew, P.A., and Cornwell, K., 2001, Two-phase heat transfer to a refrigerant in a 1 mm diameter tube, Int. J. Refrigeration, Vol. 24, pp. 51-56.

Peng X.F., and Peterson G.P., 1996, Convective Heat Transfer and Flow Friction for Water Flow in Microchannel Structures, Int. J. Heat Mass Transfer, Vol. 39, pp. 2599-2608.

Petukhov, B. S., 1970, Heat transfer and friction in turbulent pipe flow with variable physical properties, In Advances in Heat Transfer Vol. 6, Academic Press, New York, pp. 503–564.

Qu, W. and Mudawar, I., 2003, Flow boiling heat transfer in two-phase microchannel heat sinks- I. Experimental investigation and assessment of correlation methods, Int. J. Heat Mass Transfer, Vol. 46, pp. 2755-2771.

Revellin, R., Dupont, V., Ursenbacher, T. Thome, J. R., Zun, I., 2006, Characterization of diabatic two-phase flows in microchannels: Flow parameter results for R-134a in a 0.5 mm channel, Int. J. Multiphase Flow, Vol. 32, pp. 755-774.

Saitoh, S., Daiguji, H., Hihara, E., 2005, Effect of tube diameter on boiling heat transfer of R134a in horizontal small diameter tubes, Int. J. Heat Mass Transfer, Vol. 48, pp.4973-4984.

Shiferaw, D., Huo, X., Karayiannis, T.G., Kenning, D.B.R., 2007, Examination of heat transfer correlations and a model for flow boiling of R134a in small diameter tubes, Int. J Heat Mass Transfer, Vol. 50, pp. 5177-5193.

Sumith, B., Kaminaga, F., Matsumura, K., 2003, Saturated flow boiling of water in a vertical small diameter tube, Exp. Therm. Fluid Sci. Vol. 27, pp. 789–801.

Tran, T. N., Wambsganss M. W. and France D. M., 1996, Small circular- and rectangular-channel boiling with two refrigerants, Int. J. Multiphase Flow, Vol. 22, pp. 485-498.

Gnielinski, V., 1997, VDI-Wärmeatlas, Springer-Verlag, Berlin, Heidelberg.

Xu, J., Shen, S., Gan, Y., Li, Y., Zhang, W., Su, Q., 2005, Transient flow pattern based microscale boiling heat transfer mechanisms, Journal of Micromechanics and Microengineering 15, pp. 1344–1361.

Yen, T., Kasagi, N., Suzuki, Y., 2003, Forced convective boiling heat transfer in microtubes at low mass and heat fluxes Int. J. Multiphase Flow, Vol. 29, pp. 1771–1792.

Zhang, L., Koo, J., Jiang, L., Goodson, K.E., Santiago, J.G., Kenny, T.W., 2001, Study of boiling regimes and transient signal measurements in microchannels, Proc. Transducers'01, Munich, Germany, pp. 1514–1517.